Investigation of the $^{12}C+^{12}C$ $E_{c.m.}=32.5$ MeV resonance

R. A. Le Marechal, N. M. Clarke, M. Freer, B. R. Fulton, S. J. Hall, S. J. Hoad, G. R. Kelly, and R. P. Ward*
School of Physics and Space Research, University of Birmingham, Edgbaston, Birmingham B15 2TT, United Kingdom

C. D. Jones, P. Lee, and D. L. Watson
Department of Physics, University of York, Heslington, York YO1 5DD, United Kingdom

(Received 22 November 1996)

A fine-step excitation function has been measured across the resonance reported at 32.5 MeV in the $^{12}C[^{12}C,^{12}C(0_2^+)]^{12}C(0_2^+)$ reaction. Correlated structure is also observed in other exit channels involving the 0_2^+ and 3_1^- states of ^{12}C and in the $^{16}O+^{8}Be$ channel. [S0556-2813(97)03404-3]

PACS number(s): 25.70.Ef, 21.60.Gx, 27.30.+t, 27.20.+n

I. INTRODUCTION

The discovery of a resonance at $E_{c.m.}=32.5$ MeV in the $^{12}C[^{12}C,^{12}C(0_2^+)]^{12}C(0_2^+)$ reaction by Wuosmaa *et al.* [1] aroused considerable interest when it was suggested that it might be evidence for the excitation of a 6-α chain state. A number of theoretical models predict the existence of a chain state in ^{24}Mg [2–4] and calculations [5] suggest it should be found at an excitation energy some 15–20 MeV above the 6-α breakup threshold, in the excitation region in which the resonance appeared. The justification for linking the resonance observed in this decay channel to a chain state was the association of the $^{12}C(0_2^+)$ state with a highly deformed 3-α configuration, although there is evidence that it may not be a fully aligned chain state [6–12]. Further support was provided by a comparison of the ratio of the cross sections obtained in this decay channel to the $^{12}C(0_2^+)+^{12}C_{gs}$ channel with the ratio of the Coulomb penetrabilities for decay to the two channels. The differences between these suggest the decay is occurring from a highly deformed structure.

The $E_{c.m.}=32.5$ MeV resonance observed by Wuosmaa *et al.* is notable for two unusual features. It is particularly broad, with a width of 4.7 MeV, and the on-resonance angular distribution is quite distinctive, displaying large enhancements in the yield at $\theta_{c.m.}=90°$. This latter feature is very difficult to reproduce using a single partial wave. However, both of these features can be explained by a shape eigenstate model [13,14] involving the overlap of several nearly degenerate partial waves. This shape eigenstate model is compatible with the chain state interpretation.

However, an alternative explanation using the band crossing model has been proposed by Hirabayashi *et al.* [15]. They have demonstrated, using coupled channels calculations with microscopic transition densities [16], that the cross section and angular distributions can be reproduced without the need for an intermediate chain state.

More recent experimental work has provoked further controversy regarding the origin of the resonance. Resonant behavior has been reported near $E_{c.m.}=32.5$ MeV in exit channels which do not involve chainlike decay fragments [17–20]. In particular, resonances have been seen in the $^{16}O_{g.s.}+^{8}Be_{g.s.}$ and $^{12}C\,(0_2^+)+^{12}C(3_1^-)$ channels, which also display the characteristic 90° enhancement in the angular distributions. Since $^{16}O_{g.s.}$ is spherical and $^{12}C(3_1^-)$ is oblate, the observation of the resonance in these channels does not appear to be consistent with the reaction proceeding via a highly prolate intermediate state.

However, the widths of these two later resonances are narrower than the width measured by Wuosmaa *et al.* In particular, Freeman *et al.* [17] measured a width of ~ 1 MeV for the $^{16}O_{g.s.}+^{8}Be_{g.s.}$ channel which is considerably narrower than the 4.7 MeV measured by Wuosmaa *et al.* The data of Chappell *et al.* [20] for the $^{12}C(0_2^+)+^{12}C(3^-)$ channel are in fairly coarse steps across the resonance and the width is not well defined. However, it appears to be intermediate between the $^{12}C(0_2^+)+^{12}C(0_2^+)$ and the $^{16}O_{g.s.}+^{8}Be_{g.s.}$ channels. Thus the interpretation of the resonance is complicated further by the need to establish whether these later data can be linked with the original data of Wuosmaa *et al.*

To address this issue, a $^{12}C+^{12}C$ inelastic scattering experiment using a thin target was performed to investigate the energy region of the $E_{c.m.}=32.5$ MeV resonance in a series of fine energy steps. This has enabled the resonant structure in the $^{12}C(0_2^+)+^{12}C(0_2^+)$ channel to be examined in closer detail. At the same time, the resonance has also been examined in the other 6-α breakup channels $^{12}C(0_2^+)+^{12}C(3_1^-)$ and $^{12}C(3_1^-)+^{12}C(3_1^-)$, as well as the $^{16}O_{g.s.}+^{8}Be_{g.s.}$ channel and inelastic channels involving the $^{12}C_{g.s.}$ and $^{12}C(2_1^+)$ states.

II. EXPERIMENTAL METHOD

The experiment was performed at the Australian National University, using a ^{12}C beam provided by the 14UD tandem Van de Graaff facility. A laboratory energy range of 60–67.4 MeV was covered in steps of 0.2 MeV. A 14 $\mu g/cm^2$ natural carbon target foil was used, limiting the beam energy averaging to ± 15 keV.

Four position-sensitive silicon strip detectors, one pair either side of the beam, were used to detect the emerging α particles. The detectors were positioned with their centers in

*Present address: School of Sciences, Staffordshire University, College Road, Stoke-on-Trent ST4 2DE, United Kingdom.

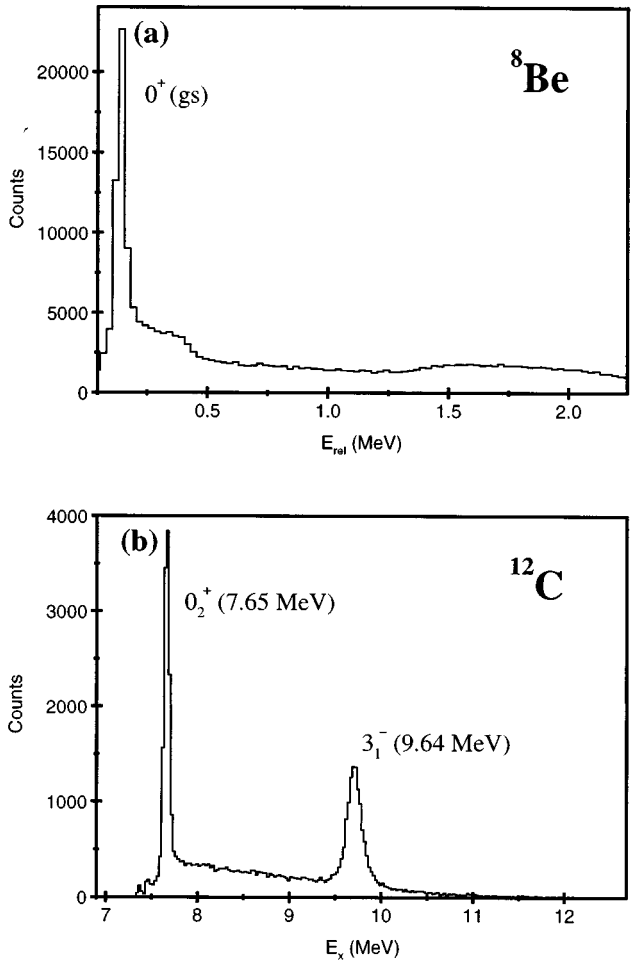

FIG. 1. (a) Spectrum showing the relative energies between each possible pair of α particles when three α particles are detected. (b) Excitation spectrum for ^{12}C, generated from the energy and position of three hits in the detectors.

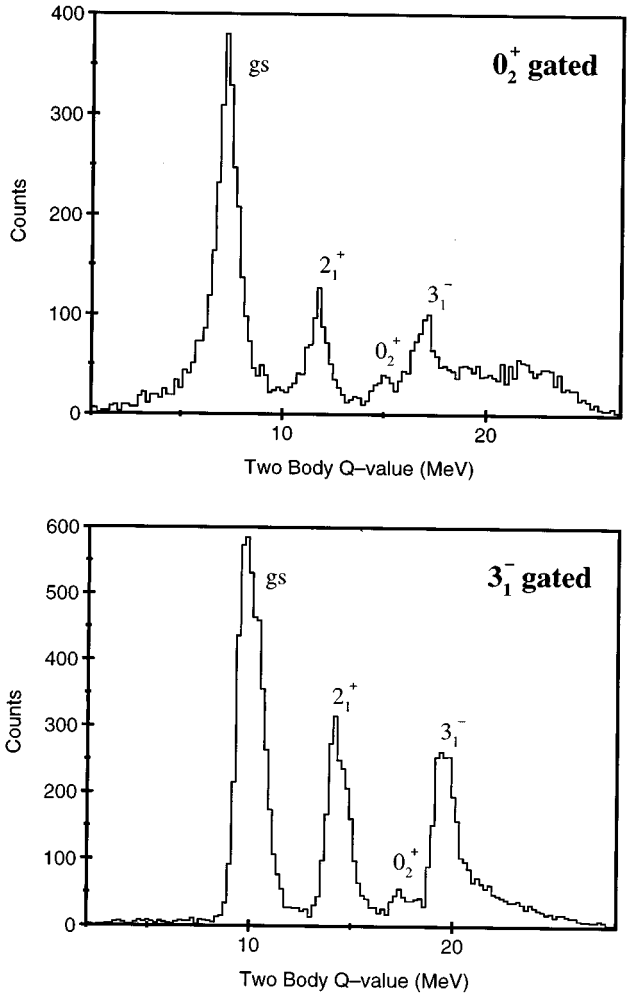

FIG. 2. Q-value spectra obtained by requiring one of the resulting ^{12}C nuclei to be (a) in the 0_2^+ state and (b) in the 3_1^- state.

plane, 12.5 cm from the target and at angles of $+24.7°$, $+51.5°$, $-31.1°$, and $-57.3°$ relative to the beam direction. Each detector had an active area of 5 cm $\times$ 5 cm and comprised 16 independent, position-sensitive strips, each 3 mm $\times$ 5 cm. This allowed the energy and position of each hit to be determined, enabling reconstruction of the event via energy and momentum conservation.

Although no explicit particle identification was made during analysis, by requiring three hits in the same pair of detectors the multiplicity was sufficiently high to keep the background level low. Moreover, because breakup from the two states of interest in ^{12}C, the 0_2^+ and the 3_1^-, proceeds largely via the ^{8}Be$+\alpha$ channel [21] the remaining background could be removed by requiring that two of the three hits originated from breakup of a ^{8}Be particle. Figure 1(a) shows the reconstructed relative energies between the three possible pairs of α particles from a triple hit in one of the detector pairs. A check was then made that one of the pairs fell in the sharp peak at 92 keV above the ^{8}Be$\rightarrow 2\alpha$ threshold.

The excitation energy of the decaying ^{12}C nucleus for such events was calculated using

$$E_x = \sum_{i=1}^{3} E_{\alpha_i} - \frac{P^2}{2M} + Q_{\text{th}}, \tag{1}$$

where the momentum of the ^{12}C nucleus P is reconstructed from the α-particle momenta P_{α_i} using

$$P^2 = \left(\sum_{i=1}^{3} P_{\alpha_i x} \right)^2 + \left(\sum_{i=1}^{3} P_{\alpha_i y} \right)^2 + \left(\sum_{i=1}^{3} P_{\alpha_i z} \right)^2 . \tag{2}$$

E_{α_i} are the energies of the α particles, Q_{th} is the threshold energy for ^{12}C breakup to three α (7.27 MeV), M is the mass of the ^{12}C. Figure 1(b) is an example of the resulting spectrum in which the 0_2^+ and 3_1^- peaks can be clearly seen. Software gates were then placed on each of these peaks and the excitation of the undetected ^{12}C calculated. Examples of the two excitation energy spectra obtained are shown in Fig. 2.

In addition, detection of double hits allowed reconstruction of ^{8}Be$+^{16}$O events in an analogous manner. The resulting ^{16}O excitation spectrum enabled investigation of the ^{16}O$_{\text{g.s.}}+^8$Be$_{\text{g.s.}}$ channel.

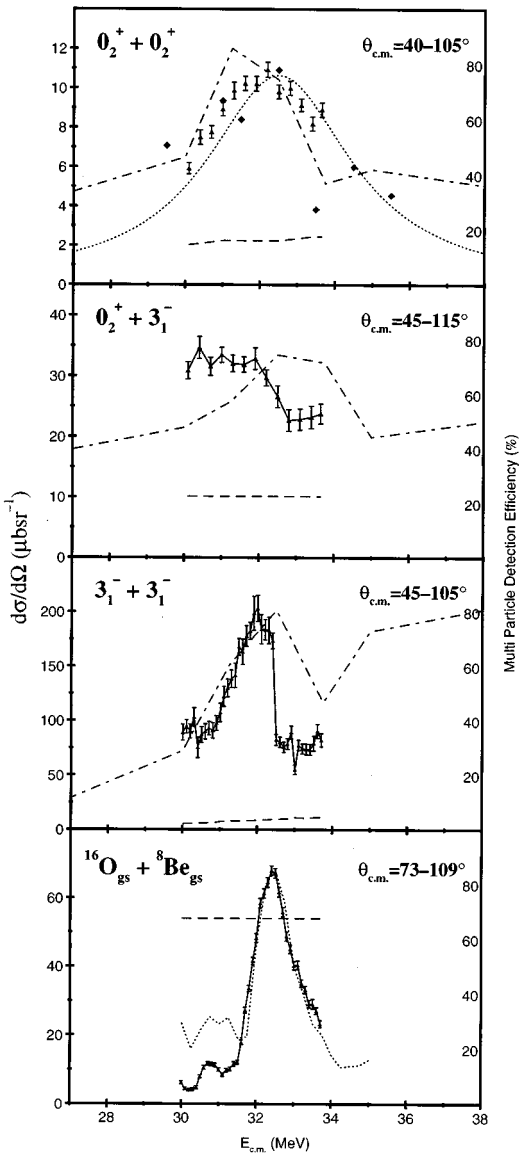

FIG. 3. Excitation functions following $^{12}C+^{12}C$ scattering for the 6-α channels over the unrestricted angular ranges indicated and the excitation function for the $^{16}O_{g.s.}+^{8}Be_{g.s.}$ channel over an angular range of $\theta_{c.m.}=73°-109°$. The dotted curve shows the data of Freeman *et al.* [17] ($\theta_{c.m.}=73°-109°$) and the dot-dashed curves show the raw data of Chappell *et al.* [20] ($\theta_{c.m.}=60°-110°$ in the $0_2^++0_2^+$ channel, $\theta_{c.m.}=65°-115°$ in the $0_2^++3_1^-$ channel and $\theta_{c.m.}=65°-115°$ in the $3_1^-+3_1^-$ channel). The earlier data of Wuosmaa *et al.* [1] ($\theta_{c.m.}=70°-105°$) is shown by a Breit Wigner curve which was fitted to the data points using the parameters defined in [1] and the diamond symbols show the later measurement ($\theta_{c.m.}=20°-105°$) [22]. Both the data sets of Wuosmaa *et al.* have been scaled by a factor of 0.7. The dashed curves show the efficiency variation in each channel.

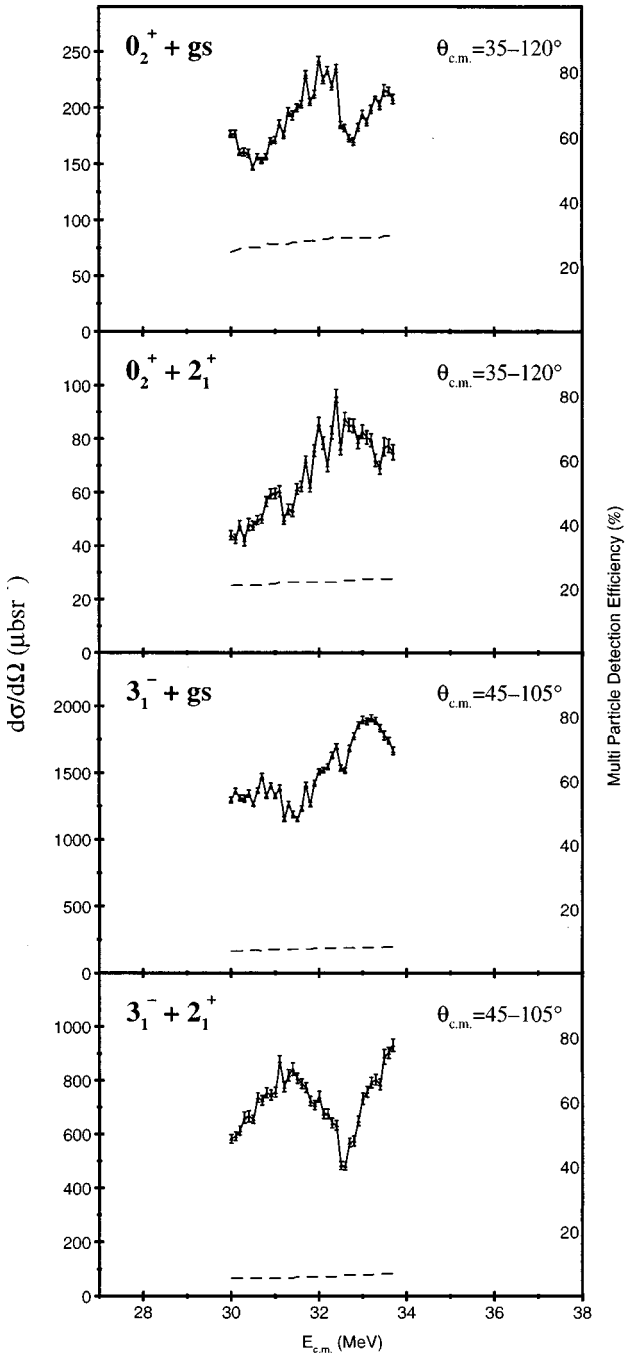

FIG. 4. Excitation functions following $^{12}C+^{12}C$ scattering for the four exit channels involving the 0_2^+ or 3_1^- state with the second ^{12}C in a bound state. The angular regions covered are indicated. The dashed curves show the efficiency variation in each channel.

III. RESULTS

Figures 3 and 4 show the excitation functions obtained for the eight exit channels investigated. The center of mass angular region covered in each channel is indicated on the figures.

A Monte Carlo simulation of the scattering and detection process was used to make efficiency corrections at each energy. A multiparticle detection efficiency was determined by comparing the efficiency for detection of three α particles after breakup with the efficiency for detection of the excited ^{12}C nucleus assuming that it remained bound. Similarly, for the detection of two α particles from a ^{8}Be nucleus. The detection simulation includes position-dependent energy thresholds and the inability to record events in which two particles strike the same strip. In all cases the calculated efficiencies vary little across the energy range (see Figs. 3, 4, 8, and 9).

The reconstruction of the data involved the detection of

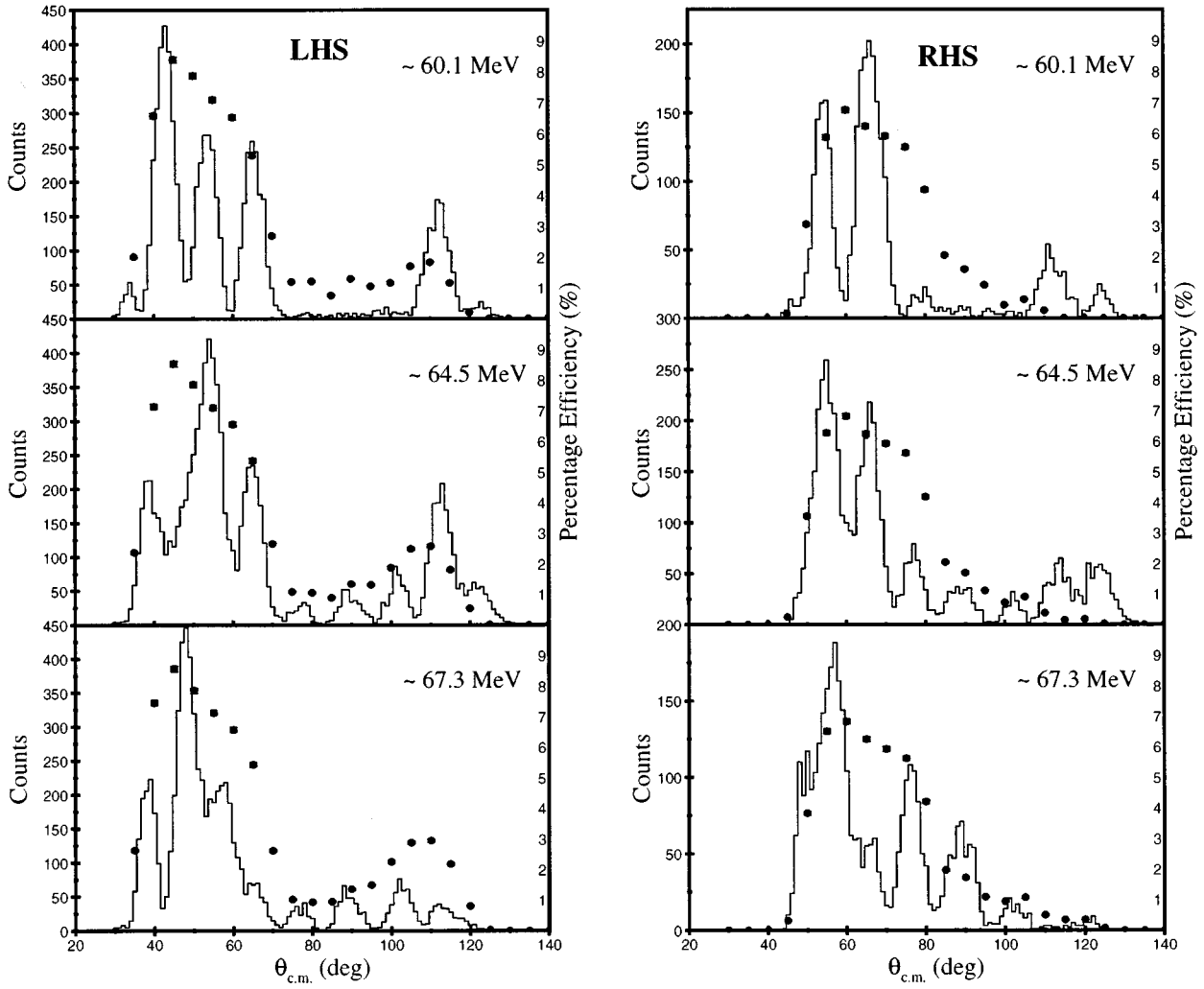

FIG. 5. Angular distributions for the $0_2^+ +$ g.s. exit channel for the left- and right-hand side detectors below, on and above resonance. The filled circles show how the efficiency varies with angle in this channel.

α particles from the breakup of only one of the two exit channel nuclei. For the symmetric channels $0_2^+ + 0_2^+$ and $3_1^- + 3_1^-$ there is double the probability for detecting the particular final state, which is not accounted for in the efficiency corrections and hence a factor of two has been divided out in these cross sections. The resulting excitation functions obtained for the three 6-α channels are shown in Fig. 3, along with that for the $^{16}O_{g.s.} + ^{8}Be_{g.s.}$ channel.

Due to the low yield in the $0_2^+ + 0_2^+$ and $0_2^+ + 3_1^-$ channel, the data for each set of three adjacent energies have been summed. In this case, the efficiency has been calculated for the middle energy, but typically changes by <1 % between the three energies.

The resonance in the $0_2^+ + 0_2^+$ channel appears very similar to previous measurements, although the cross sections measured here are about 70% of the values measured by Wuosmaa *et al.* Therefore, the data of Wuosmaa *et al.* have been scaled in order to make comparison of the two data sets easier. The solid curve represents the earlier measurement covering an angular range of 70–105 [1], and the diamond symbols a later measurement covering a somewhat larger angular range ($\theta_{c.m.} = 20° - 105°$) [22]. There is a reasonable agreement in the present data with these measurements and with the data of Chappell *et al.* [20] (dot-dashed curve on figure).

By contrast, the $0_2^+ + 3_1^-$ channel appears not to show the structure observed in the measurement of Chappell *et al.* [20] (dot-dashed curve on figure). However, it should be noted that this measurement covers a wider angular range.

The most interesting result is the very striking resonance in the $3_1^- + 3_1^-$ channel. Previous evidence for resonant structure was observed in the data of Chappell [23], prior to making efficiency corrections (dot-dashed curve on figure). However, this new measurement reveals the resonance to be considerably narrower, with a width of around 1.5 MeV, and there is no evidence for fine structure.

The data for the $^{16}O_{g.s.} + ^{8}Be_{g.s.}$ channel have been restricted to the angular range $\theta_{c.m.} = 73° - 109°$ as covered in the measurements of Freeman *et al.* (dotted curve on the figure). There is very good agreement between the two measurements and again there is no evidence for fine structure. It should, however, be noted that the electronics setup was primarily designed to detect multiplicity 3 events which resulted in some difficulty in calculating the cross sections in this channel. To overcome this problem, the data were normalized to the data in Ref. [19] at $\theta_{c.m.} = 90°$ on resonance.

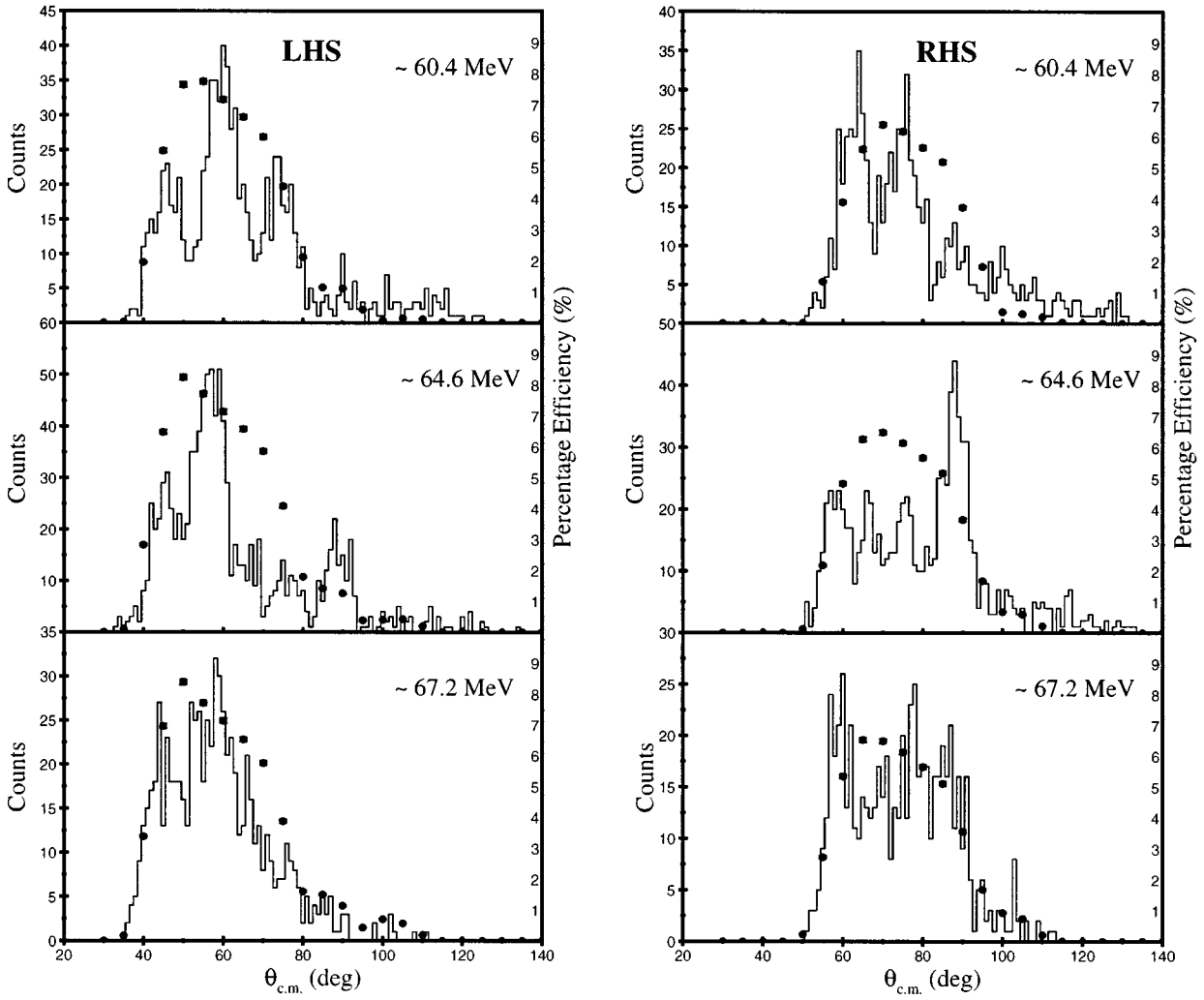

FIG. 6. Angular distributions for the $0_2^+ + 0_2^+$ exit channel for the left- and right-hand side detectors show, on and above resonance. The filled circles show how the efficiency varies with angle in this channel.

As a result, there may be some degree of systematic error in this channel, and detailed comparisons of cross-sections between this and other channels may not be possible.

Figure 4 shows the excitation functions for the four channels involving the 0_2^+ or 3_1^- state in association with the second ^{12}C in a bound state [either the ground state (g.s.) or the 2_1^+]. Two of these are relatively featureless, but the $0_2^+ +$ g.s. channel again shows a noticeable resonance at just above $E_{c.m.}=32$ MeV with a width of around 1.5 MeV and, interestingly, there is a prominent dip in the $3_1^- + 2_1^+$ channel at the same energy.

Angular distributions for those channels with spin zero particles are shown in Figs. 5–7 for three energies below, on and above the resonance energy. Because of the low yield in the $0_2^+ + 0_2^+$ channel, three adjacent energy runs have been summed for the on and above resonance spectra and five energies for the below resonance spectrum. Similarly, for the $0_2^+ +$ g.s. channel and $^{16}O_{g.s.}+^{8}Be_{g.s.}$ two adjacent energy runs have been summed for each spectrum. The filled circles show the detection efficiency as a function of angle. Oscillatory structure is clearly defined in all three channels and in the case of the $0_2^+ + 0_2^+$ and $^{16}O_{g.s.}+^{8}Be_{g.s.}$ channels, the previously noted on-resonance enhancements at 90° and $\sim 54°$ [22] are clearly visible. The data are not sufficiently sensitive to confirm any such enhancement in the $0_2^+ +$ g.s. channel. Angular distributions in the channels with nonzero spin are not shown here as the structure is less well defined.

The observation that the resonance appeared particularly in the yield around 90° suggested that measurements around this angular region might be more sensitive to the resonance. In order to investigate this, we have reanalyzed the existing data over a restricted angular range between 70–105°. This also allowed a more direct comparison of the present measurements with the earlier measurement of Wuosmaa *et al.* and provided a comparison of the different exit channels over the same angular range. Figure 8 shows the resulting excitation functions for the three 6-α channels.

Although there is little significant difference in the profile of the resonance in either the $0_2^+ + 0_2^+$ and $3_1^- + 3_1^-$ channels, the $0_2^+ + 0_2^+$ appears to follow the trend in the earlier measurement of Wuosmaa *et al.* more closely. As before, there is a difference in the cross sections of the two sets of data and that of Wuosmaa *et al.* has been scaled. (Wuosmaa *et al.* reported an on-resonance cross section of 15 μb sr^{-1}.) In the $0_2^+ + 3_1^-$ channel, there is now an indication of a similar

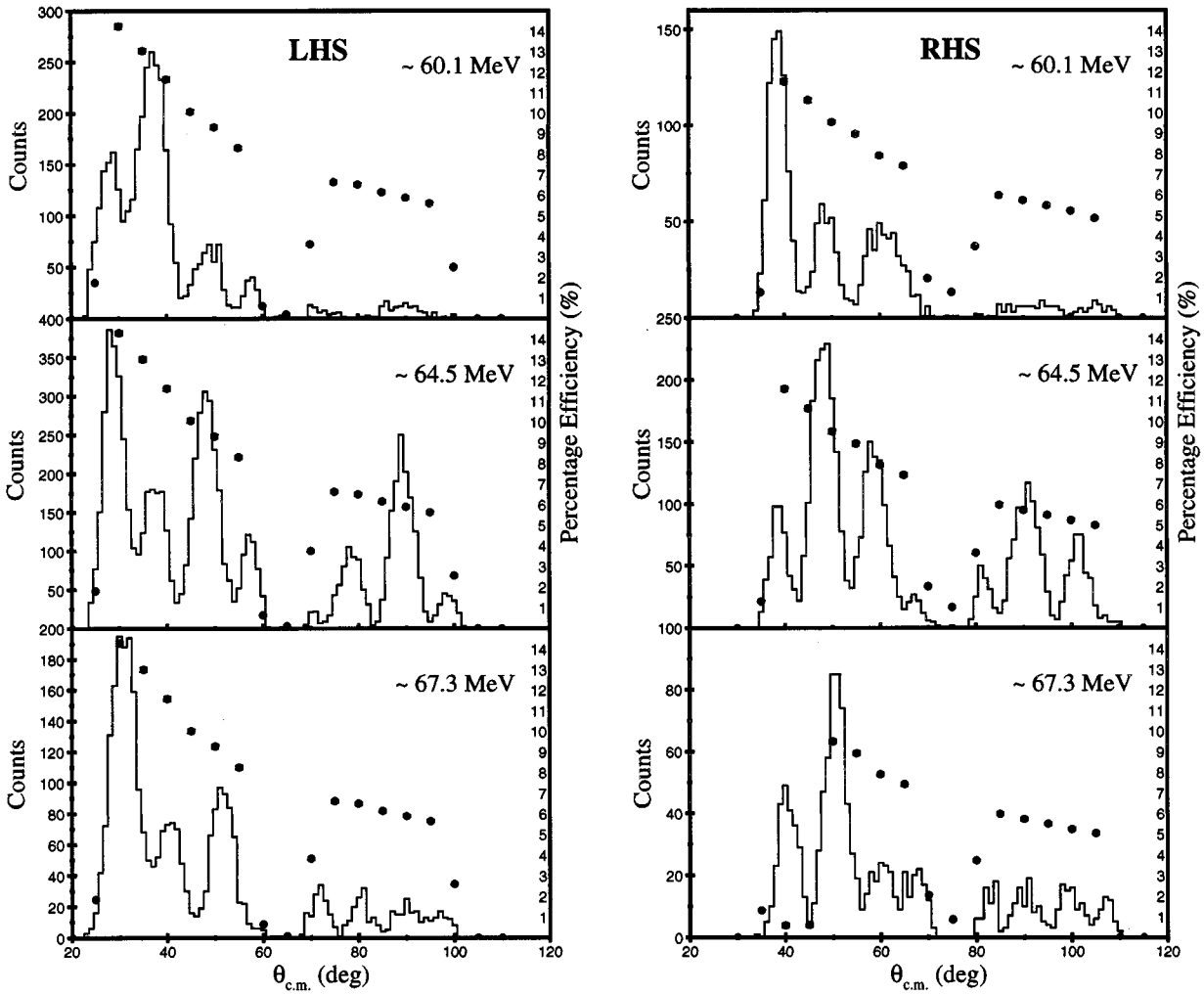

FIG. 7. Angular distributions for the $^{16}O_{g.s.}+^{8}Be_{g.s.}$ exit channel for the left- and right-hand side detectors below, on and above resonance. The filled circles show how the efficiency varies with angle in this channel.

structure which was not apparent in the excitation function taken from the wider angle data set.

The effect of this restriction in angular coverage in channels involving the ground state or 2_1^+ state is shown in Fig. 9. A comparison of the excitation functions obtained from the restricted angular range (Fig. 9) with the wider angle range shows the resonance in the $0_2^+ + \text{g.s.}$ channel to be even narrower (500 keV), with a similar narrow (0.5–1 MeV) structure appearing in the $0_2^+ + 2_1^+$ channel. There is also weaker evidence for this structure in the $3_1^- + \text{g.s.}$ channel.

IV. DISCUSSION

The most dramatic aspect of the present measurements is that the resonance at $E_{\text{c.m.}}=32.5$ MeV previously observed in the $0_2^+ + 0_2^+$ channel appears very strongly in a number of other inelastic channels, in particular the $3_1^- + 3_1^-$ and $0_2^+ + \text{g.s.}$ channels. In addition, there is evidence for structure in further channels $0_2^+ + 3_1^-$, $0_2^+ + 2_1^+$, and $3_1^- + \text{g.s.}$ if the angular region investigated is restricted to around 90°. Furthermore, the width of the resonance is very narrow (1.0–1.5 MeV) in several of these channels, and even narrower (0.5 MeV in the $0_2^+ + \text{g.s.}$ channel) in the restricted angular range measurements.

Whether or not all the observed structures arise from a common resonance is still open to debate. This measurement shows the structures to all appear at the same energy. Furthermore, the similarity of the angular distributions in the $0_2^+ + 0_2^+$ and $^{16}O_{g.s.}+^{8}Be_{g.s.}$ channels and the enhancement in structure around the 90° region in these and other channels appears to provide a common link. Conversely, the discrepancy in widths may cast doubt on this link. However, if the enhancement in the yield does arise from a true resonance, it is possible for the apparent width and position of the resonance to vary in different exit channels and in different angular regions, depending on the degree of background yield with which the resonant yield can interfere. In which case, the variation in the width of the structures observed as the angular coverage is changed must reflect interference with a different background yield. This observation greatly complicates our task of interpreting the data, in particular because the present thin target data do not cover a sufficient energy range for the background level to be identified in all the channels. Moreover, in such circumstances total cross-

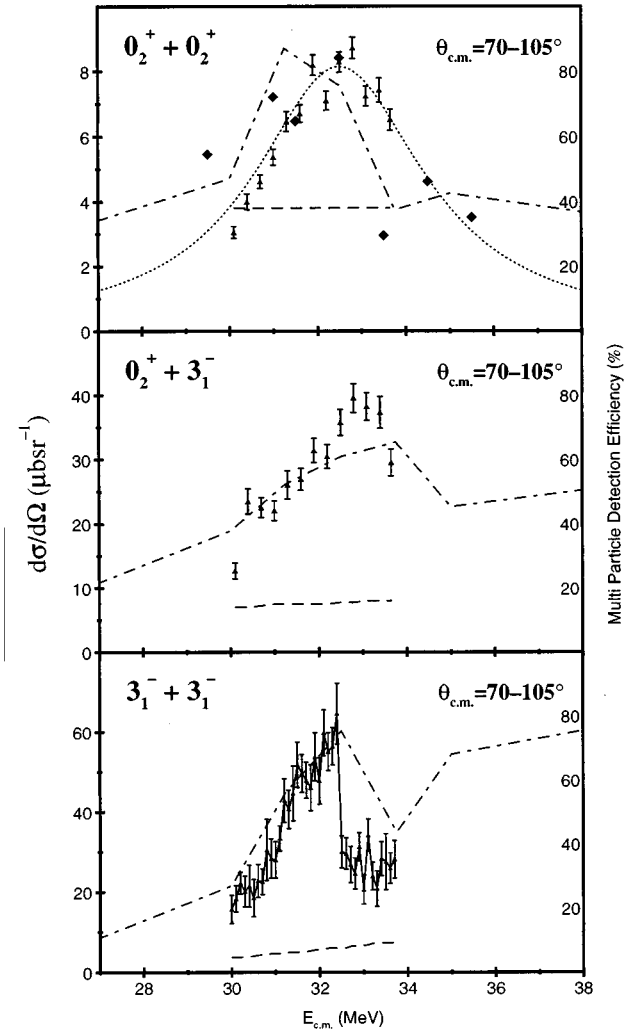

FIG. 8. Excitation functions for the 6-α channels over an angular range of $\theta_{c.m.}=70°-105°$. The dotted curves show the data of Wuosmaa *et al.* [1] ($\theta_{c.m.}=70°-105°$) and the dot-dashed curves show that of Chappell *et al.* [20] ($\theta_{c.m.}=60°-110°$ in the $0_2^+ + 0_2^+$ channel, $\theta_{c.m.}=65°-115°$ in the $0_2^+ + 3_1^-$ channel and $\theta_{c.m.}=65°-115°$ in the $3_1^- + 3_1^-$ channel). The later data of Wuosmaa *et al.* [22] ($\theta_{c.m.}=20°-105°$) is shown by the diamond symbols. Both the data sets of Wuosmaa *et al.* have been scaled by a factor of 0.7. The dashed curves show the efficiency variation in each channel.

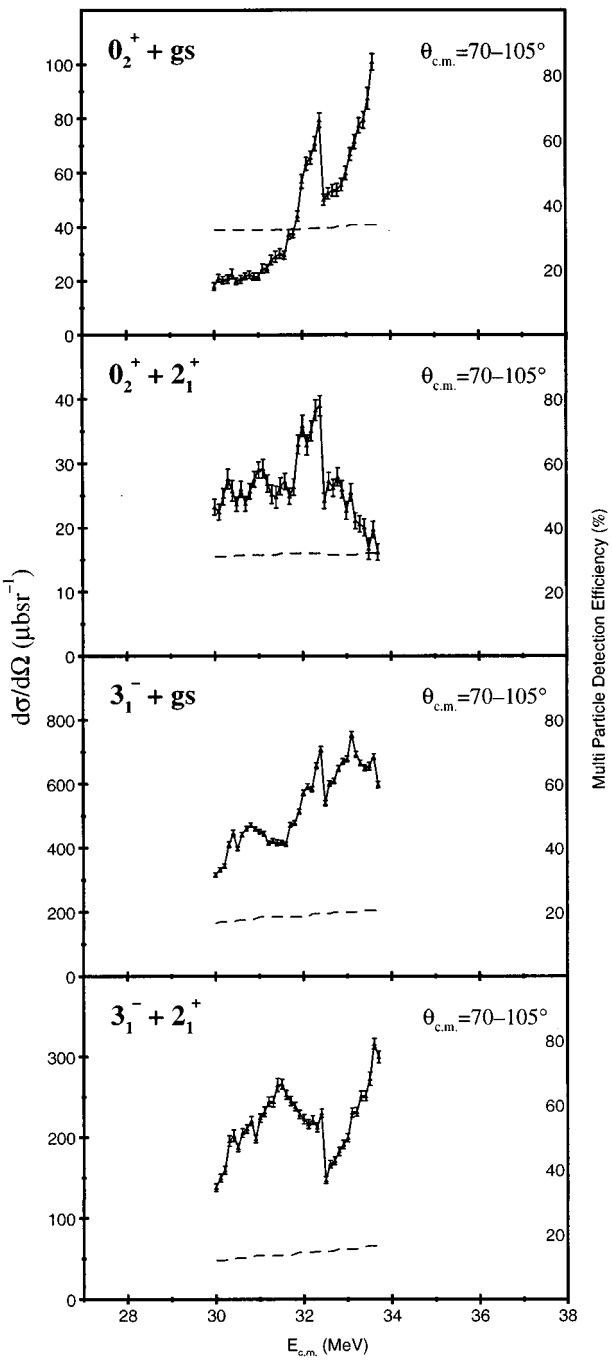

FIG. 9. Excitation functions over an angular range of $\theta_{c.m.}=70°-105°$ for the four exit channels involving the 0_2^+ or 3_1^- state with the second ^{12}C in a bound state. The dashed curves show the efficiency variation in each channel.

section data is needed, requiring a full angular coverage. Even with such an extensive data set, a comprehensive interpretation of the structures seen in all the channels in terms of direct and resonant processes would be difficult as the reaction processes leading to the background will probably be very different in the low lying (well matched) channels and the higher channels.

If we do assume that the structures observed arise from a common resonance, the strength in the different channels must in some part be reflected by the different decay penetrabilities in each channel. Table I shows the relative Coulomb penetration factors for each channel calculated assuming a channel radius of $1.4(A_1^{1/3}+A_2^{1/3})$ and angular momenta of 12, 14, and 16. For decay involving nonzero channel spin, full alignment is assumed. To some extent the different channel strengths in the restricted angular region do appear to be consistent with the trend shown in the penetration factors. However, the magnitude of difference between these factors for the different channels varies with angular momentum, precluding a conclusive interpretation.

V. SUMMARY

Previous measurements have reported a dramatic resonance in the $^{12}C[^{12}C,^{12}C(0_2^+)]^{12}C(0_2^+)$ reaction at $E_{c.m.}=32.5$ MeV. The present work shows that structure is

TABLE I. Comparison of the Coulomb penetrabilities of the exit channels under investigation.

		a		
1	$P(0_2^+ + \text{g.s.})/P(\text{g.s.})$	$P(0_2^+ + 2_1^+)/P(\text{g.s.})$	$P(0_2^+ + 0_2^+)/P(\text{g.s.})$	$P(0_2^+ + 3_1^-)/P(\text{g.s.})$
12	0.71	0.71	0.19	0.46
14	0.53	0.54	0.039	0.21
16	0.27	0.27	0.0043	0.048
		b		
1	$P(3_1^- + \text{g.s.})/P(\text{g.s.})$	$P(3_1^- + 2_1^+)/P(\text{g.s.})$	$P(3_1^- + 3_1^-)/P(\text{g.s.})$	$P(^{16}\text{O}_{\text{g.s.}} + ^8\text{Be})/P(\text{g.s.})$
12	0.96	0.95	0.69	0.95
14	0.92	0.91	0.50	0.88
16	0.82	0.79	0.24	0.75

also observed at the same energy in a number of other inelastic scattering channels. The width of the resonance is very narrow (1.5 MeV) in some of them and the appearance of structure is enhanced in the 90° region.

The measurements point to the difficulties in interpreting coincidence data taken over a limited range of angular coverage. Without a sufficiently extensive measurement it is possible that the yield will not reflect the total cross section in the various channels, making the extraction of partial widths difficult. Moreover, the measured position and width of a structure may not correctly reflect the true position and width of the resonance. The continuing development of large detector arrays will help in this respect.

The nature of the exit channels in which the resonance is observed make the formation of an intermediate chain state appear unlikely since a number of them have no structural overlap with highly deformed prolate shapes. On the other hand, the narrow width of the resonances also poses problems for the band crossing model interpretation [15]. A weak coupling model such as this must include couplings to many more channels in order to reproduce widths of around 1 MeV. In particular, it would be of interest to see how the inclusion of the $^{16}\text{O}_{\text{g.s.}} + ^8\text{Be}_{\text{g.s.}}$ channel affects the calculation. An alternative explanation has been suggested [24,25], following the observation of structure in the $3_1^- + 3_1^-$ channel. The proposed mechanism is based upon a resonance process involving the $3_1^- + 3_1^-$ channel, similar to that involved in the dramatic resonances observed in the $2_1^+ + 2_1^+$ channel [26]. The striking resonance in this channel appears to provide some support for this model. However, the variety of channels in which prominent structure is observed suggest that further investigation of these resonances is required before any conclusions can be made.

ACKNOWLEDGMENTS

This work was carried out under a formal agreement between the U.K. Engineering and Physical Sciences Research Council (EPSRC) and Australian National University (ANU). The authors thank the staff at ANU for their help. G. R. Kelly, M. Freer, S. J. Hoad, and P. Lee acknowledge support from the EPSRC.

[1] A. H. Wuosmaa, R. R. Betts, B. B. Back, M. Freer, B. G. Glagola, Th. Happ, D. J. Henderson, and P. Wilt, Phys. Rev. Lett. **68**, 1295 (1992).
[2] G. Leander and S. E. Larsson, Nucl. Phys. **A239**, 93 (1975).
[3] H. Flocard, P. H. Heenen, S. J. Kreiger, and M. S. Weiss, Prog. Theor. Phys. **72**, 1000 (1984).
[4] W. Bauhoff, H. Schultheis, and R. Schultheis, Phys. Lett. **95B**, 5 (1980); **106B**, 278 (1981); Phys. Rev. C **22**, 861 (1980); **29**, 1046 (1984).
[5] S. Marsh and W. D. M. Rae, Phys. Lett. B **180**, 185 (1986).
[6] H. Morinaga, Phys. Rev. **101**, 254 (1956); Phys. Lett. **21**, 78 (1966).
[7] D. M. Brink, H. Freidrich, A. Weiguny, and C. Wong, Phys. Lett. **33B**, 143 (1970).
[8] N. Takigawa and A. Arima, Nucl. Phys. **A168**, 593 (1971).
[9] H. Freidrich, L. Sapathy, and A. Weiguny, Phys. Lett. **36B**, 189 (1971).
[10] N. De Takacsy, Nucl. Phys. **A178**, 469 (1972).
[11] Y. Suzuki, H. Horiuchi, and K. Ikeda, Prog. Theor. Phys. **47**, 1517 (1972).
[12] C. Bargoltz, Nucl. Phys. **A243**, 449 (1975).
[13] W. D. M. Rae, A. C. Merchant, and B. Buck, Phys. Lett. B **69**, 3709 (1992).
[14] A. C. Merchant and W. D. M. Rae, J. Phys. G **19**, L89 (1993).
[15] Y. Hirabayashi, Y. Sakuragi, and Y. Abe, Phys. Rev. Lett. **74**, 4141 (1995).
[16] M. Kamimura, Nucl. Phys. **A351**, 456 (1981).
[17] R. M. Freeman, F. Haas, A. Elanique, A. Morsad, and C. Beck, Phys. Rev. C **51**, 3504 (1995).
[18] E. T. Mirgule, Suresh Kumar, M. A. Eswaran, D. R. Chakra-

barty, V. M. Datar, N. L. Ragoowansi, H. H. Oza, and U. K. Pal, Nucl. Phys. **A583**, 287 (1995).

[19] M. Aliotta, S. Cherubini, E. Costanzo, M. Lattuada, S. Romano, D. Vinciguerra, and M. Zadro, Z. Phys. A **353**, 43 (1995); M. Aliotta, S. Cherubini, E. Costanzo, M. Lattuada, S. Romano, C. Spitaleri, D. Vinciguerra, and M. Zadro, *ibid.* **354**, 119 (1996); Nucl. Phys. **A583**, 281 (1995).

[20] S. P. G. Chappell, D. L. Watson, S. P. Fox, C. D. Jones, W. D. M. Rae, P. M. Simmons, M. Freer, B. R. Fulton, N. M. Clarke, N. Curtis, M. J. Leddy, J. S. Pople, S. J. Hall, R. P. Ward, G. Tungate, W. N. Catford, G. J. Gyapong, S. M. Singer, and P. H. Regan, Phys. Rev. C **51**, 695 (1995).

[21] M. Freer, A. H. Wuosmaa, R. R. Betts, D. J. Henderson, P. Wilt, R. W. Zurmühle, D. P. Balamuth, S. Barrow, D. Benton, Q. Li, Z. Liu, and Y. Miao, Phys. Rev. C **49**, R1751 (1994).

[22] A. H. Wuosmaa, M. Freer, B. B. Back, R. R. Betts, J. C. Gehring, B. G. Glagola, Th. Happ, D. J. Henderson, P. Wilt, and I. G. Bearden, Phys. Rev. C **50**, 2909 (1994).

[23] S. P. G. Chappell, Ph.D. thesis, University of York, U.K., 1995.

[24] W. D. M. Rae, P. E. Fry, and A. C. Merchant, J. Phys. G **22**, L13 (1996).

[25] S. P. G. Chappell and W. D. M. Rae, Phys. Rev. C **53**, 2879 (1996).

[26] T. M. Cormier, C. M. Jachcinski, G. M. Berkowitz, P. Braun-Munzinger, P. M. Cormier, M. Gai, J. W. Harris, J. Barrette, and H. E. Wegner, Phys. Rev. Lett. **40**, 924 (1978); T. M. Cormier, J. Applegate, G. M. Berkowitz, P. Braun-Munzinger, P. M. Cormier, J. W. Harris, C. M. Jachcinski, L. L. Lee, Jr., J. Barrette, and H. E. Wegner, *ibid.* **38**, 940 (1980).